

Preparation and Characterization of Polyimide composites with Layered double hydroxides

Pingchuan Ma (马平川), Yuchun Song, Zhenghui Yang, Furong Li, Haiquan Guo* (郭海泉), Lianxun Gao

Lab of Polymer Composites Engineering, Changchun Institute of Applied Chemistry, Chinese Academy of Sciences, Changchun, 130022, P.R. of China (中国科学院长春应用化学研究所)

E-mail address: hqguo@ciac.ac.cn

Abstract: Layered double hydroxide (LDHs) was modified with 4-amino benzoate via anion-exchange intercalated procedure. The interlayer spacing was expanded from 0.76 nm to 1.50 nm, leading to the stacking Mg/Al nano-layers easily exfoliated in polymer matrix to form nanocomposites. Amino benzoate modifying layered double hydroxides/polyimide nanocomposites (LDH-AM/PI) were prepared through in situ polymerization. The SEM and XRD were used for investigating the Mg/Al nano-layers dispersion behavior. The mechanical and thermal properties were improved effectively by the incorporation of Mg/Al nanolayers in PI matrix.

Keywords: Nanocomposite; Polyimide; Layered double hydroxide

1. INTRODUCTION

Due to excellent dielectric, thermal and mechanical properties, aromatic polyimides are considered to be one of the most useful super-engineering plastics and have various applications in the microelectronics and motors as insulating materials [1-3]. Recently, with the development of some new technologies, such as low loss tangent are required [2,4-6]. However, it is difficult for neat PI films to meet the requirements. To overcome these, many kinds of PI/inorganic materials nanocomposites with performance superior to those of pure PI have been fabricated.

Layered double hydroxides (LDHs) belong to the group of clay minerals that exhibit many potential applications including adsorbents, anion exchangers, pollutant adsorption, electrochemical capacitor, flame retardants, the formation of interesting nano-composite materials [7-13]. LDHs were first discovered by Hochstetter in Sweden in 1842 and prepared nano-composite materials with LDHs by Park in 1989 [14,15]. However, when using LDHs as filler, the big challenge is LDHs were inclined to agglomeration in the polymer matrix, because they are incompatible. Generally, the existence of interfacial bonding between the LDHs and polymer matrix leads to the inorganic and organic phases being dispersed at the nanometer level, which can exhibit more excellent performance than conventional composites [16-18].

In this study, layered double hydroxide ($\text{Mg}_6\text{Al}_2(\text{OH})_{16}\text{CO}_3 \cdot 4\text{H}_2\text{O}$) was modified with 4-amino benzoate via anion-exchange intercalated procedure, and then LDH-AM of different contents were introduced into PI matrix to prepare composite films via in situ polymerization. The microstructure of neat PI and PI/LDH-AM were characterized by scanning electron microscopy. The change of mechanical and thermal properties are caused by LDH-AM were investigated.

2. EXPERIMENTAL

2.1 Materials

The LDHs and 4-amino benzoic acid were purchased from Sigma-Aladdin Chemical. Nitric acid (HNO₃) was supplied by Yantai Yuandong Co. Ltd. 4,4'-Oxydianiline (ODA) and Pyromellitic dianhydride (PMDA) was purchased Shandong Wanda Chemical Co. Ltd. N,N-Dimethylacetamide (DMAc) was obtained from Beijing Chemical Works and distilled over calcium hydride under reduced pressure.

2.2 Preparation of LDH-AM

The LDHs and 4-amino benzoic acid were dispersed in deionized water. HNO₃ was mixed with the above solution dropwise and continue stirred for 72 h. The LDH-AM was obtained after filtering, washing and drying treatments.

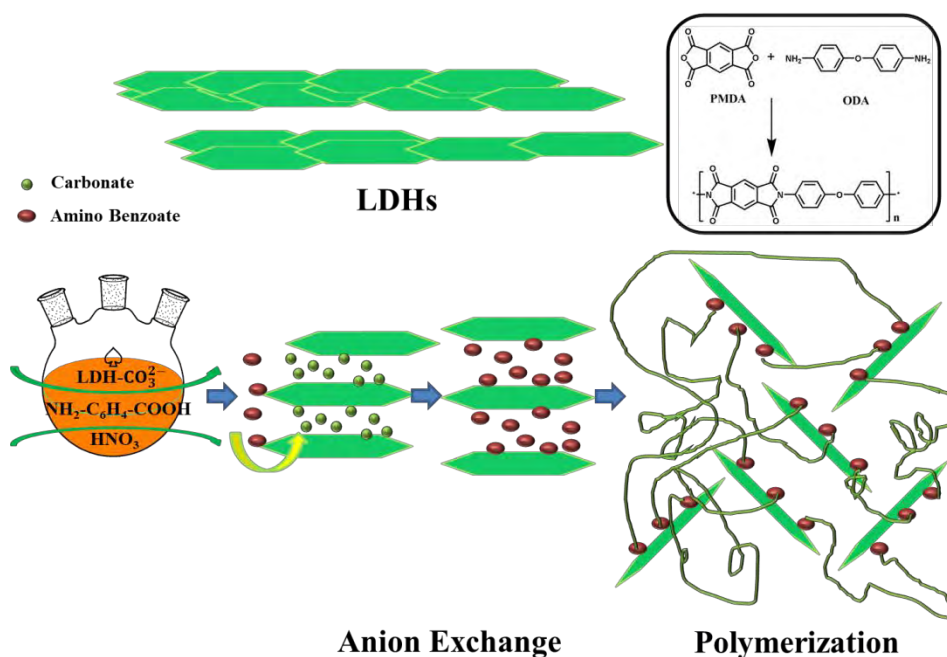
2.3 Preparation of PI/LDH-AM Composite films

Typically, ODA and LDH-AM were thoroughly dissolved in DMAc in a three-necked round bottom flask at room temperature by ultrasonic treatment for 4 hours. PMDA was sequentially mixed with the above mixture solution at 0 °C under N₂ atmosphere. The above solution was kept continuously stirred at room temperature for 24 h to obtain viscous PAA/LDH-AM solution. The above solution was cast onto a glass substrate by auto film applicator, and then thermally treated at 80 °C for 3 h, 150 °C for 1 h, 250 °C for 1 h, 350 °C for 1 h and 400 °C for 2 h to obtain a series of PI/LDH-AM composite films. The thickness of the films was about 25 μm.

To interpret the formation mechanism of PI/LDH-AM composite films prepared, the synthesise procedure is shown in Scheme 1. First, amino benzoate insert the interlayer galleries of LDHs to substitute carbonate, and the ion exchanging reaction could happen, the interlayer space was expanded. And then, PMDA was added ODA/LDH-AM/DMAc solution, one anhydride group of PMDA reacted with the amine of LDH-AM and the another anhydride group reacted with ODA. Finally, the polymerization was occurred in the interlayer galleries.

2.4 Characterization

Fourier transform infrared spectra (FT-IR) were obtained on a Bruker Vertex 70 FTIR spectrometer. The crystal structure was determined by the wide-angle X-ray diffractometer (WXR D, Rigaku D/max 2500 PC) with Cu K_α irradiation ($\lambda = 1.5418 \text{ \AA}$, $2\theta = 2\text{--}50^\circ$). Mechanical properties of composite films were measured using a universal testing apparatus (INSTRON-1121) with a strain speed of 5 mm min⁻¹ at room temperature. The morphologies of LDH-AM powder and fracture surface of PI/LDH-AM films were investigated with field emission scanning electron microscope (XL30 ESEM FEG) with an accelerating voltage of 5 kV. The thermogravimetric analysis (TGA) was performed using a TGA analyzer (PerkinElmer TGA-2) with the heating rate of 10 °C min⁻¹ under N₂. The dynamic mechanical analysis (DMA) of the hybrid films was conducted with Rheometric Scientific Inc Dynamic Mechanical Analyzer at a heating rate of 10 °C min⁻¹.



Scheme 1 Preparation of PI/LDH-AM composites.

3. RESULTS AND DISCUSSION

3.1 Characterization of LDH-AM

XRD plays an important role in determining the morphological features of any compound. The XRD patterns of LDH- CO_3^{2-} and LDH-AM are shown in Figure 1. The XRD pattern of LDH- CO_3^{2-} reveals the characteristic intense diffraction peak at $2\theta=11.6^\circ$, which corresponded to the basal spacing with the d spacing of 7.4 Å. When LDH- CO_3^{2-} intercalated by 4-amino benzoate, two peaks are present at $2\theta=5.8^\circ$ and $2\theta=11.6^\circ$ for LDH-AM, indicating that the interlayer space is expanded from 7.4 Å to 15.2 Å. Meanwhile, the diffraction peak at $2\theta=11.6^\circ$ is attributed to (006) crystal plane of LDH-AM rather than (003) of LDH- CO_3^{2-} .

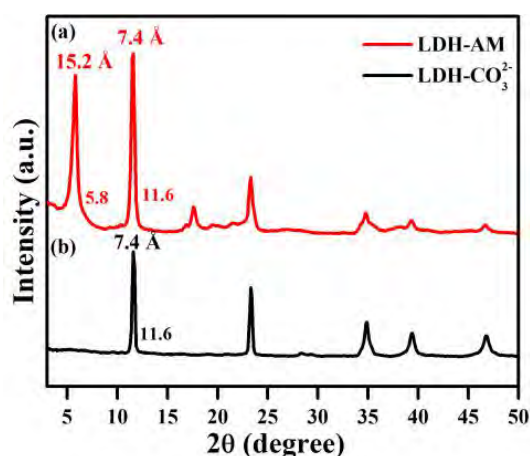


Figure 1 XRD patterns of (a) LDH-AM and (b) LDH- CO_3^{2-} .

To prove above conjecture, the FTIR spectra of LDH-AM and LDH- CO_3^{2-} are compared. As shown in Figure 2. FTIR of LDH-AM exhibit strong absorption at 1530 and 1397 cm^{-1} , corresponding to asymmetric and symmetric vibration of $-\text{COO}^-$, respectively^[19]. The peaks exist at 1612 and 1594 cm^{-1} , which are attributed to N-H bend and aromatic C=C stretching, respectively^[13]. Interestingly, the characteristic absorption peak of $-\text{CO}_3^{2-}$ at 1369 cm^{-1} disappeared in LDH-AM, indicating that 4-amino benzoate completely replaces carbonate insert the laminate of LDHs.

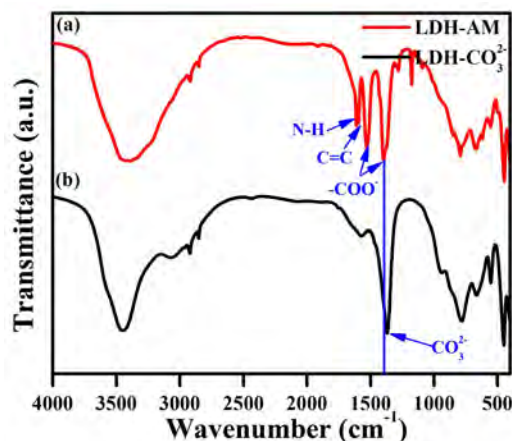


Figure 2 FTIR spectra of (a) LDH-AM and (b) LDH- CO_3^{2-} .

3.2 Characterization of nanocomposite films

The FTIR spectra of neat PI and PI/LDH-AM films are shown in Figure 3. The absorption peaks at 1776, 1715 and 722 cm^{-1} are corresponded to asymmetric stretching, symmetric stretching and bending vibrations of C=O, respectively. Aromatic C=C stretching appears at 1594 cm^{-1} while C-N stretching appears at 1368 cm^{-1} . The characteristic absorption peaks of PAA at 1660 cm^{-1} and 1550 cm^{-1} are not observed, indicating that the imidization of neat PI and PI/LDH-AM films are complete. Interestingly, the peaks at 1612 cm^{-1} of N-H disappeared in all PI/LDH-AM composite films, which can be explained that PMDA molecules insert into interlayer galleries to react with amine group of LDH-AM, and then polymerization to form PAA/LDH-AM solution.

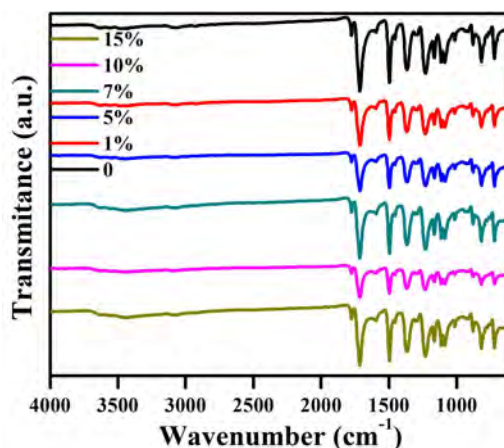


Figure 3 FTIR spectra of neat PI and PI/LDH-AM films.

Figure 4 show the XRD patterns of neat PI film and PI/LDH-AM composites films with the different

LDH-AM contents. From this figure, only broad peaks could be observed at about 18-22° in spite of LDH-AM content, which corresponding to the characteristic diffraction peak of neat PI. Comparing with Figure 3(b)-3(e), we could find that with the increase of LDH-AM content from 1 wt% to 15 wt%, no diffractions of LDH-AM are detected. Above results indicate that the Mg/Al nano-layers of LDH-AB were well dispersed in the PI matrix.

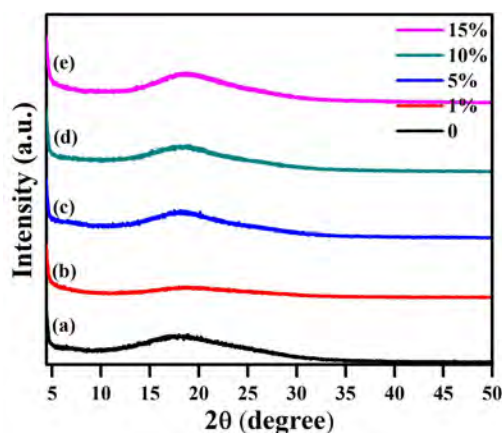


Figure 4 XRD patterns of neat PI and PI/LDH-AM films.

The morphology of neat PI and PI/LDH-AM films are shown in Figure 5. The fractured surface of pure PI is very smooth and flat in 5(a), while the fractured surface of composite films are comparatively rougher. Furthermore, LDH-AM sheets are homogenously dispersed and embedded in the PI matrix with LDH-AM contents below 7 wt% (Figure 5(b-d)), due to the LDH-AM interlinked with the PI through covalent bonding, enhancing the compatibility between the filler and matrix. However, when overfull LDH-AB content are added (more than 7 wt%), the Mg/Al nano-layers are aggregated in PI matrix (Figure 5(e-f)), which representing a defect to influence the properties of composite films.

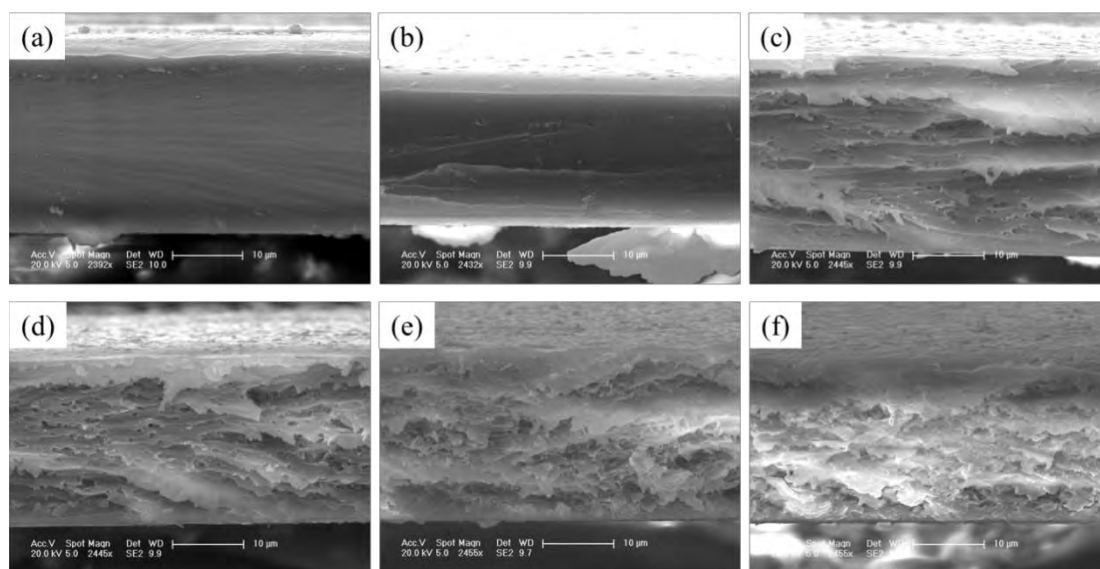


Figure 5 SEM images of the fracture surface of (a) neat PI, (b) PI/1wt% LDH-AM, (c) PI/5wt% LDH-AM, (d) PI/7wt% LDH-AM, (e) PI/10wt% LDH-AM, (f) PI/15wt% LDH-AM.

The mechanical properties of neat PI and related nanocomposites with different contents of LDH-AM (1-15 wt%) are summarized in Table 1, the variations of Tensile strength, Elongation at break and Young's modulus of films are shown in Figure 6. The increment of tensile strength is increased with the LDH-AM. The tensile strain of composite film with 5 wt % LDH-AM is most increased contrast with neat polyimide.

The main explanation for the improvement in tensile strain in PI nanocomposite is the good compatibility between PI matrix and Mg/Al nano-layers via formation of chemical bond of the clay edges. At high LDH-AM loading (more than 5 wt %), Mg/Al nano-layers may aggregate together to form a defect and deteriorate tensile strength. Furthermore, the elongation at break of the PI/LDH-AM composite films increased with the LDH-AM content. With 5 wt% of LDH-AM content, the elongation at break is 63%, which is 135% higher than neat PI. By the same reasoning, the elongation behavior of the PI/LDH-AM films is also determined by the interfacial bonding between the Mg/Al nano-layers and the PI matrix. When the LDH-AM content more than 5 wt%, the elongation is reduced, due to some aggregation of the Mg/Al nano-layers has occurred. The Young's modulus of the PI/LDH-AM composite films increases with LDH-AM content increase, because rigid LDH nano-layers well dispersed in PI matrix enhance these nanocomposites tenacity.

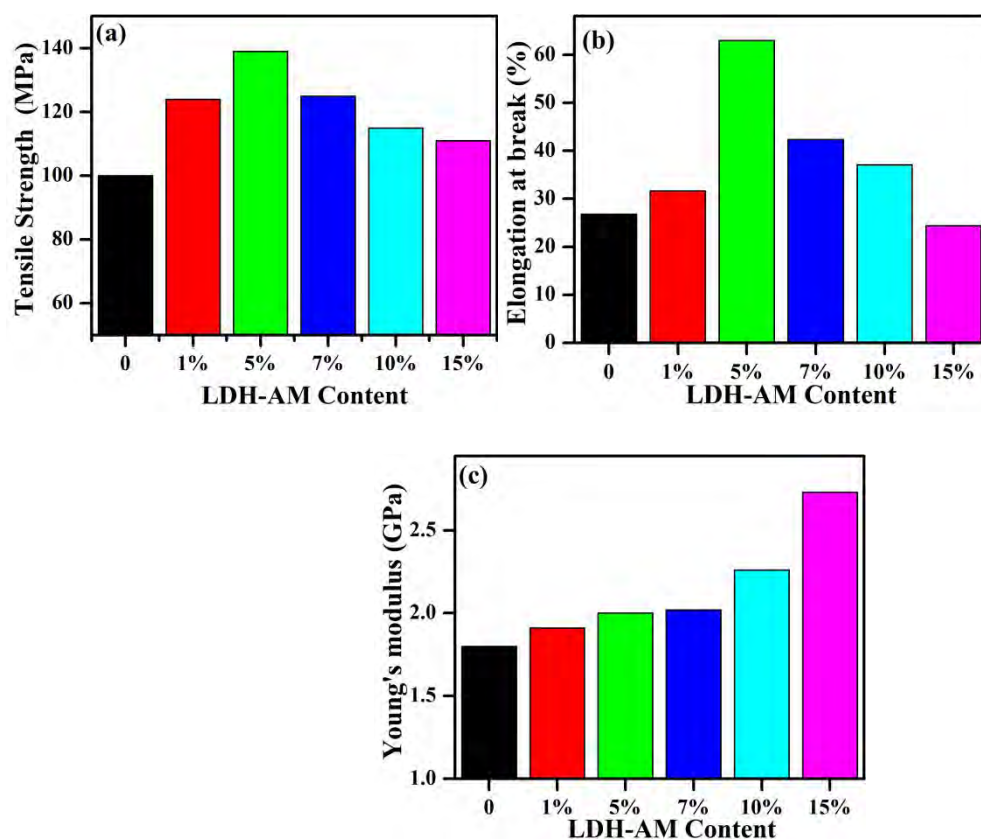


Figure 6 Variations of Tensile strength (a), Elongation at break (b) and Young's modulus (c) of neat PI and PI/LDH-AM composite films.

Table 1 Mechanical Properties of neat PI and PI/LDH-AM composite films.

Material	Tensile strength (MPa)	Elongation at break (%)	Young's modulus (GPa)
Neat PI	100	26.8	1.80
1%	124	31.6	1.91
5%	139	63.0	2.00
7%	125	42.3	2.02
10%	115	37.1	2.26
15%	111	24.4	2.73

TGA was used to study the thermal stability of the PI/LDH-AM composite films. Figure 7(a) display the TGA and DTG curves of LDH-AM. The LDH-AM decomposition in three distinct regions could be observed. The region I in the temperature range of 50–200 °C was associated with the interlayers and physically adsorbed water, constituting about 4.92% weight loss. Region II from 200 °C to 314 °C was related to partial dehydroxylation of the metal hydroxide layers, contributed to about 3.87% of the weight loss. Region III between 314 °C and 570 °C was due to the decomposition of 4-amino benzoate, gave a weight loss of about 43.27%. The TGA curves of neat PI and PI/LDH-AM composite films are shown in Figure 7(b) and the dates are summarized in Table 2. At 10% weight loss (T_{d10}), neat PI film has a decomposition temperature of 591 °C under nitrogen atmosphere. By adding LDH-AM, T_{d10} of the composite films are overall reduced. The reduction in thermal resistance with increasing LDH-AM is ascribed to the decomposition of LDH. This trend is somewhat different from that observed from Hsueh’s report [13]. At 15 wt% LDH-AM content, T_{d10} of composite film is 564 °C, and find that only 4.6% reduce for these composite films, indicating that PI/LDH-AM composite films have better thermal stability.

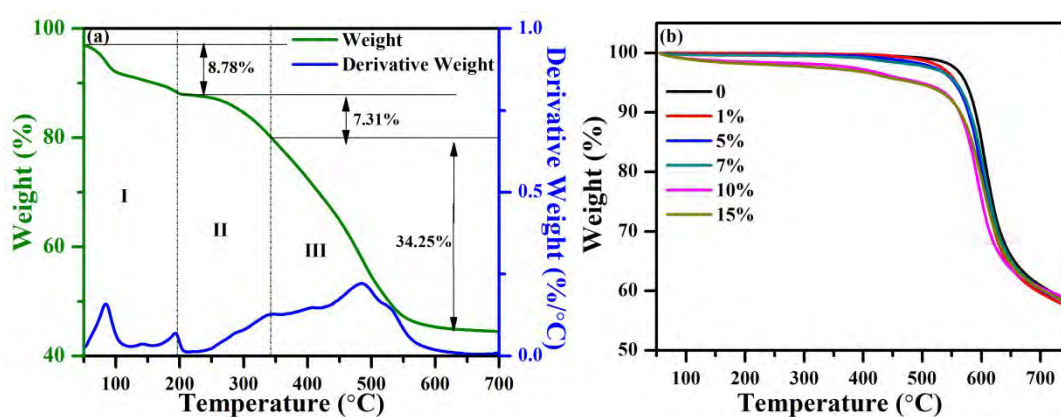


Figure 7 TGA and DTG curves of LDH-AM (a), and TGA curves of neat PI and PI/LDH-AM composite films.

The glass transition temperature (T_g) and coefficient of thermal expansions (CTE) of neat PI and PI/LDH-AM composite films were analyzed by DMA and TMA, and the detail date are summarized in Table 2. It was note-worthy that LDH-AM could bring in a significant improvement in storage modulus (E') because the covalent bonds between LDH-AM and polyimide enhanced the interfacial adhesion. The T_g values of PI/LDH-AM films are improved with increasing LDH-AM content, which can be attributed that more well dispersed LDH nano-layers hinder PI chain mobility and rotation because the strong interaction is existed between LDH-AB and PI molecules. Meanwhile, the $\tan\delta$ values are associated with the molecular chain mobility. The LDH-AM added into PI chain restricts the molecular mobility and in turn decreases the values of $\tan\delta$. Its $\tan\delta$ values lower than neat PI indicating that the rigidity of film is increased when the PI matrix containing LDH-AM.

Table 2 Thermal properties of neat PI and PI/LDH-AM composite films.

Material	DMA			TGA	
	E' (MPa)	T_g (°C)	$\tan\delta$	T_{d5} (°C)	T_{d10} (°C)
Neat PI	1094	393	0.2747	573	591
1%	1574	410	0.2480	557	590
5%	1737	412	0.2325	554	578
7%	2002	413	0.2348	549	577
10%	2602	418	0.2056	496	565
15%	2976	421	0.1898	487	564

References

- [1] Tsai, M.-H.; Wang, H.-Y.; Lu, H.-T.; Tseng, I. H.; Lu, H.-H.; Huang, S.-L.; Yeh, J.-M., Properties of polyimide/Al₂O₃ and Si₃N₄ deposited thin films. *Thin Solid Films*, **2011**, *519*, 4969-4973.
- [2] Wang, T.; Wang, M.; Fu, L.; Duan, Z.; Chen, Y.; Hou, X.; Wu, Y.; Li, S.; Guo, L.; Kang, R.; Jiang, N.; Yu, J., Enhanced Thermal Conductivity of Polyimide Composites with Boron Nitride Nanosheets. *Sci Rep*, **2018**, *8*, 1557.
- [3] Li, H.; Liu, G.; Liu, B.; Chen, W.; Chen, S., Dielectric properties of polyimide/Al₂O₃ hybrids synthesized by in-situ polymerization. *Materials Letters*, **2007**, *61*, 1507-1511.
- [4] Uera, K., Polyimide, polyamic acid and processes for the production thereof. **2013**.
- [5] Wu, D.; Niu, H.; Qi, S.; Han, E.; Yan, X.; Tian, G.; Wu, Z.; Wang, X.; US: 2016.
- [6] Liu, F.; Liu, Z.; Gao, S.; You, Q.; Zou, L.; Chen, J.; Liu, J.; Liu, X., Polyimide film with low thermal expansion and high transparency by self-enhancement of polyimide/SiC nanofibers net. *Rsc Advances*, **2018**, *8*.
- [7] Gore, C. T.; Omwoma, S.; Chen, W.; Song, Y. F., Interweaved LDH/PAN nanocomposite films: Application in the design of effective hexavalent chromium adsorption technology. **2016**, *284*, 794-801.
- [8] Chubar, N.; Gilmour, R.; Gerda, V.; Mičušík, M.; Omastova, M.; Heister, K.; Man, P.; Fraissard, J.; Zaitsev, V., Layered double hydroxides as the next generation inorganic anion exchangers: Synthetic methods versus applicability. *Adv Colloid Interface Sci*, **2017**, *245*, 62-80.
- [9] Malak-Polaczyk, A.; Vix-Guterl, C.; Frackowiak, E., Carbon/Layered Double Hydroxide (LDH) Composites for Supercapacitor Application†. *Energy & Fuels*, **2010**, *24*.
- [10] Tzou, Y. M.; Wang, S. L.; Hsu, L. C.; Chang, R. R.; Lin, C., Deintercalation of Li/Al LDH and its application to recover adsorbed chromate from used adsorbent. *Applied Clay Science*, **2007**, *37*, 107-114.
- [11] Becker, C. M.; Gabbardo, A. D.; Wypych, F.; Amico, S. C., Mechanical and flame-retardant properties of epoxy/Mg-Al LDH composites. *Composites Part A Applied Science & Manufacturing*, **2011**, *42*, 196-202.
- [12] Mallakpour, S.; Dinari, M.; Hatami, M., Modification of Mg/Al-layered double hydroxide with L-aspartic acid containing dicarboxylic acid and its application in the enhancement of the thermal stability of chiral poly(amide-imide). *Rsc Advances*, **2014**, *4*, 42114-42121.
- [13] Hsueh, H. B.; Chen, C. Y., Preparation and properties of LDHs/polyimide nanocomposites. *Polymer*, **2003**, *44*, 1151-1161.
- [14] Park, I. Y.; Kuroda, K.; Kato, C., Preparation of a layered double hydroxide-porphyrin intercalation compound. *Chemistry Letters*, **1989**, *11*, 2057-2058.
- [15] †, C. H., Ueber Bleiweissbildung. *Journal Für Praktische Chemie*, **26**, 338-353.
- [16] Dinari, M.; Nabiyan, A., Citric acid - modified layered double hydroxides as a green reinforcing agent for improving thermal and mechanical properties of poly(vinyl alcohol) - based nanocomposite films. *Polymer Composites*, **2016**, n/a-n/a.
- [17] Jinhee, A.; Mijeong, H.; Chang - Sik, H., Preparation and characterization of polyimide/modified layered double hydroxide nanocomposites. *Polymer International*, **2010**, *60*, 271-278.
- [18] Lv, F.; Wu, Y.; Zhang, Y.; Shang, J.; Chu, P. K., Structure and magnetic properties of soft organic ZnAl-LDH/polyimide electromagnetic shielding composites. *Journal of Materials Science*, **2011**, *47*, 2033-2039.
- [19] Li, Y.; Tang, L.-P.; Zhou, W.; Wang, X.-R., Fabrication of intercalated p -aminobenzoic acid into Zn-Ti layered double hydroxide and its application as UV absorbent. *Chinese Chemical Letters*, **2016**, *27*, 1495-1499.